

Early Cretaceous radiolarians from the Indus suture zone, Ladakh, northern India

KOJIMA Satoru*, Talat AHMAD**#, TANAKA Tsuyoshi#,
Triloki Nath BAGATI**, Miwnal MISHRA**,
Rohtash KUMAR**, Rafiqul ISLAM** and Prampal KHANNA**

Abstract The Nidar ophiolitic complex in eastern Ladakh, northern India, consists of ultramafic rocks, gabbro and sedimentary-volcanic member, in ascending order. The sedimentary-volcanic member in the Nidar area is about 370 m in thickness, and is composed of alternating chert, jasperite, volcanic rocks, red shale, volcanic conglomerate, sandstone and shale. Among these rocks, chert and shale yields well-preserved radiolarian fossils, which range in age, at least, from Hauterivian to Aptian (Early Cretaceous). These ages are consistent with the Sm-Nd mineral-whole rock isochron age of the underlying gabbro. The lithology, ages and geochemical characteristics of the Nidar ophiolitic complex indicate that the complex formed in an intra-oceanic volcanic arc setting. A chert block from the Shergol ophiolitic melange in western Ladakh yields Albian radiolarians.

Key words: Cretaceous, radiolarians, Shergol ophiolitic melange, Nidar ophiolitic complex, Indus suture zone, Ladakh, India

Introduction

Geologic history of the Neo-Tethys ocean was recorded in the rocks of the Indus suture zone (ISZ), or the Indus-Tsangpo suture zone, which is traced, at least, from Tibet in the east to Pakistan in the west (Fig. 1). The ocean is generally considered to open in the Triassic and close in the Eocene (e.g., Dewey et al., 1988; Searle, 1991). The precise history, however, is controversial among researchers (e.g., Beck et al., 1995; Rowley, 1996) partly because of the regional differences in geology and reconstructed paleogeography along the suture zone. In order to make the development of the whole of the Neo-Tethys clear, we need detailed geologic data all along the suture.

The Ladakh Himalaya in the western part of the ISZ is one of the suitable place to study the geology of the ISZ. Basic geologic and paleontologic data of the Ladakh Himalaya, however, are scarce, especially in its eastern part.

* Department of Civil Engineering, Gifu University, Gifu 501-1193, Japan

** Wadia Institute of Himalayan Geology, P.O. Box 74, Dehradun 248 001, India

Department of Earth and Planetary Sciences, Nagoya University, Nagoya 464-8602, Japan

In this paper, we report radiolarian fossils from the sedimentary-volcanic member of the Nidar ophiolitic complex in eastern Ladakh and the chert block in the Shergol ophiolitic melange in western Ladakh. We also discuss the age and depositional setting of the Radiolaria-bearing rocks. This is the first report of radiolarian fossils from eastern Ladakh.

Geologic Setting

The Ladakh Himalaya is subdivided into the Karakoram zone, Shyok suture zone, ISZ and Zaskar zone from NE to SW (Thakur, 1981; Figs. 1-3). Northeastern part of the ISZ is occupied mostly by the Late Cretaceous to Late Tertiary Ladakh plutonic complex. But the country rock of this pluton includes Paleozoic rocks, and the Ladakh plutonic complex or the Ladakh block is interpreted to be a fragment of continent (Robertson and Degnan, 1994). The Shyok suture zone represents the paleo-ocean between the Karakoram and Ladakh blocks or continents. To the south of the Ladakh block, a variety of Mesozoic to Cenozoic sedimentary-igneous rock complexes occur forming narrow belts: they are interpreted to be deposited in the Neo-Tethys oceanic basin or to be originated as part of the intra-oceanic volcanic arc within the Neo-Tethys.

In the western Ladakh, rocks of the ISZ are subdivided

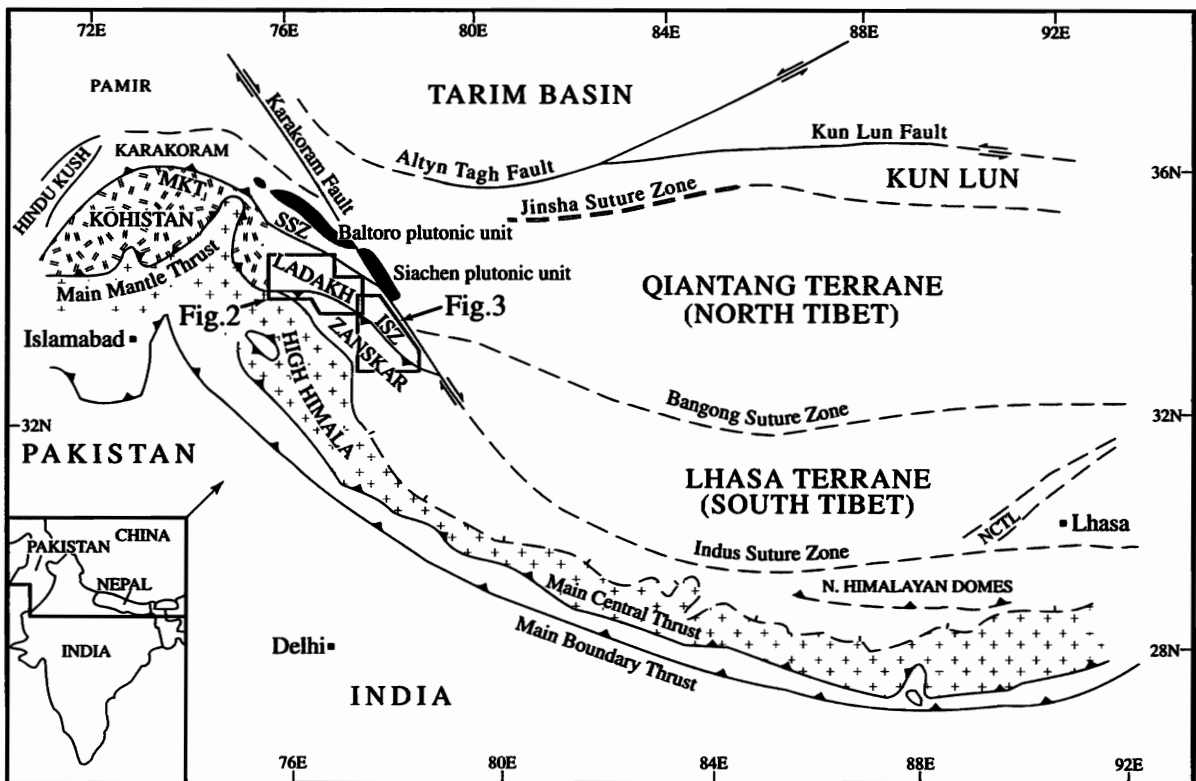


Fig. 1. Map showing the tectonic subdivision of the Himalayan Range and locations of Figs. 2 and 3. MKT: Main Karakoram thrust, SSZ: Shyok suture zone, ISZ: Indus suture zone, NCTL: Nyenchen Tanggla Range. Modified from Searle et al. (1999).

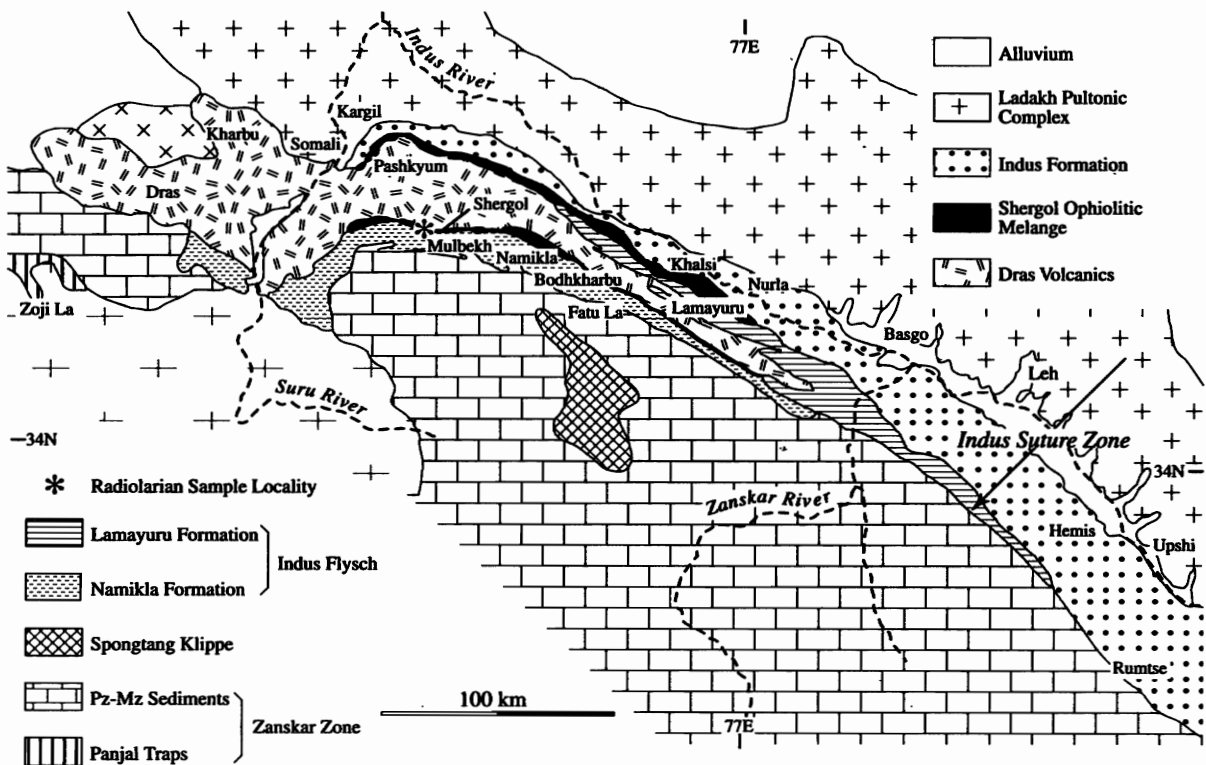


Fig. 2. Geologic map of the western Ladakh Range. After Sinha and Mishra (1992).

into the Namikla Formation, Lamayuru Formation, Dras volcanics, Shergol ophiolitic melange and Indus Formation (Fig. 2). According to the geologic and tectonic reconstruction by Sinha and Mishra (1992), Sinha and Upadhyay (1993), Robertson and Degnan (1994), Upadhyay and Sinha (1998) and Clift et al. (2000), these geologic units are interpreted as follows; The Namikla and Lamayuru Formations are deep-water passive margin sediments on the Indian plate, and are Triassic to Eocene in age (Upadhyay and Sinha, 1998). The Jurassic to Cretaceous Dras volcanics

were accumulated in the intra-oceanic arc, which is correlated with the Kohistan arc in Pakistan (Fig. 1). The Shergol ophiolitic melange was formed by the northward subduction of Neo-Tethys ocean beneath the Eurasian (Ladakh-Karakoram) continent. The age of the melange is considered to be Jurassic to Late Cretaceous on the basis of foraminiferal and radiolarian fossils (Shah and Sharma, 1977; Upadhyay and Sinha, 1998). The samples treated for the radiolarian analysis in this paper are chert blocks in the Shergol ophiolitic melange. The Tertiary Indus Formation

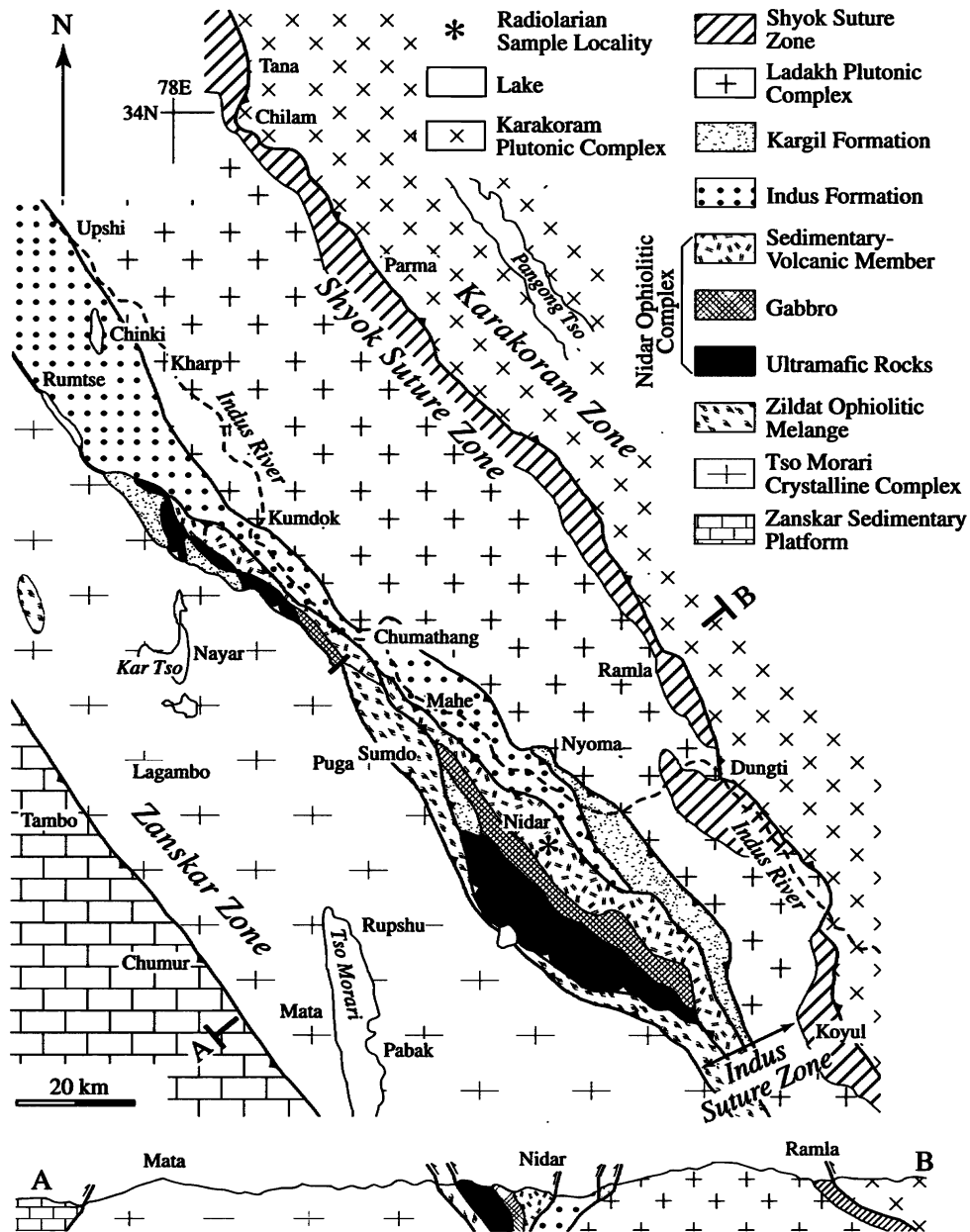


Fig. 3. Geologic map of the eastern Ladakh Range. Simplified from Ahmad et al. (1996).

or Indus Molasse is the products of collision between India and Eurasia.

The ISZ in eastern Ladakh is composed of the Zildat ophiolitic melange, Nidar ophiolitic complex, Indus Formation, Kargil Formation and Ladakh plutonic complex (Fig. 3). The Zildat ophiolitic melange is interpreted to be formed by subduction of the Neo-Tethys ocean, and is correlated with the Shergol ophiolitic melange in western Ladakh (Ahmad et al., 1996). The Nidar ophiolitic complex consists of ultramafic rocks, gabbro and sedimentary-volcanic member in ascending order; namely the complex has an ophiolite succession. The sedimentary-volcanic member is well exposed in the Nidar area (Fig. 3), and is composed of chert, jasperite, shale, siltstone, sandstone, gritty sandstone, conglomerate, volcanic tuff, pyroclastic rocks, volcanogenic sandstone and volcanic rocks (Fig. 4; Bagati and Kumar, 1999). In the lower part of the section shown in Fig. 4, radiolarian chert is a dominant facies, whereas sandstone, siltstone and shale are dominant in the middle part. In the upper part of the section, major part of the rocks are represented by conglomerate and volcanic rocks with some thrust sheets of gabbro intervening between these rocks. Samples treated in this paper were collected from this section, and their horizons are shown in Fig. 4. The Kargil Formation consists mainly of conglomerate, sandstone and minor shale interlayers yielding Neogene fossils such as freshwater molluscs, plant remains and a vertebrate (Thakur, 1981).

Early Cretaceous radiolarians

The rock samples including chert, siliceous shale and shale from the Nidar ophiolitic complex in eastern Ladakh and the Shergol ophiolitic melange in western Ladakh were treated with 5 % hydrofluoric acid. We used the treatment method developed by Pessagno and Newport (1972). All the fossil individuals reported in this paper are deposited in the Nagoya University Museum, and the radiolarian photomicrographs are stored in the Earth Science Laboratory, Department of Civil Engineering, Gifu University. All the figures in Plates 1-5 are numbered, for example, as 123/NDC-56, whose numerator represents a sequential number of SEM (scanning electron microscope) photomicrograph and the denominator indicates the rock specimen number shown in Figs. 4 and 5. Identification and systematics of the radiolarians are mainly based on the study by Baumgartner et al. (1995), supplementary referring to Schaaf (1981),

O'Dogherty (1994) and others.

1. Radiolarians from the Nidar ophiolitic complex and their ages

We collected and treated 33 siliceous sedimentary rock samples from the sedimentary-volcanic member of the Nidar ophiolitic complex (Figs. 3 and 4), 16 samples of which yield radiolarians well-preserved and abundant enough to determine the ages (Figs. 4 and 5; Plates 1-5). In this paper we assume that the section measured near Nidar and shown in Fig. 4 is continuous on the basis of the lithologic continu-

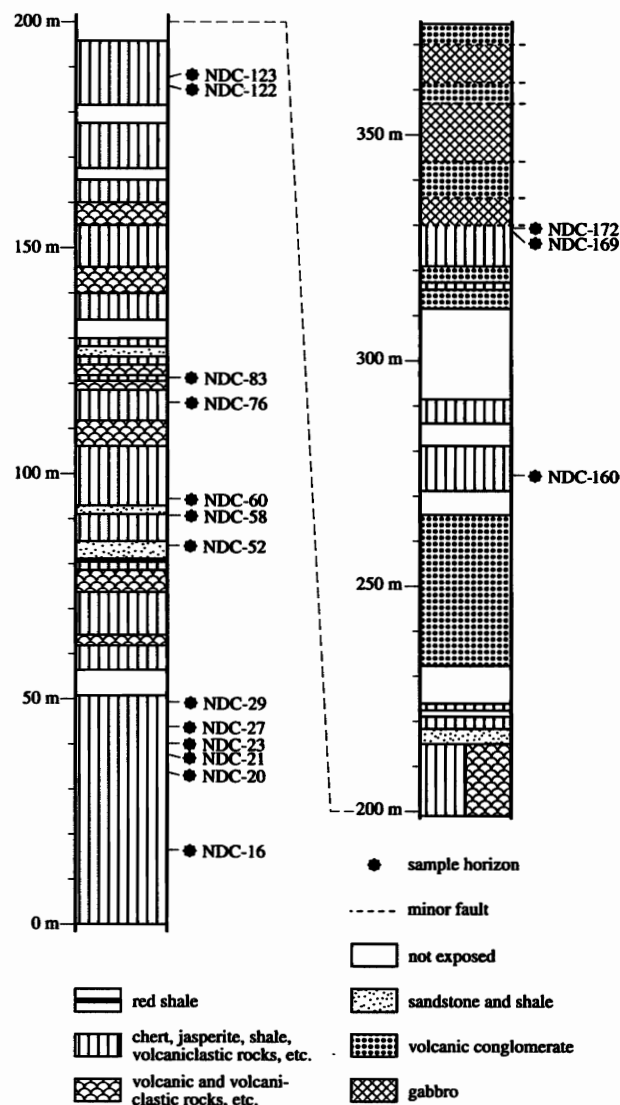


Fig. 4. Columnar section of the Nidar sedimentary-volcanic member indicating the horizons of the Radiolaria-bearing samples. Locality of the section is indicated in Fig. 3 as radiolarian sample locality. Simplified from Bagati and Kumar (1999).

ity, although there are some horizons not exposed.

Most of the radiolarians from the Sample NDC-16 have long ranges, and it is difficult to determine the age precisely. However, occurrence of *Cecrops septemporatus* and *Hemicryptocapsa capita* are restricted from late Valanginian to early Barremian and late Valanginian to early Hauterivian, respectively (Schaaf, 1984; Sanfilippo and Riedel, 1985; Baumgartner et al., 1995). First appearance horizon of *Dictyomitra pseudoscalaris* is also late Valanginian (Baumgartner et al., 1995). Concurrence of these species strongly indicates that the age of the Sample NDC-16 is late Valanginian or Hauterivian. Occurrence of *Pseudodictyomitra nuda*, *Sethocapsa* sp. cf. *S. uterculus*, *Thanarla pulchra* and *Wrangellium puga* also supports this age estimation. By the assumption that the section examined is continuous, by the occurrence of similar radiolarian species, and by the age of the Sample NDC-29 (see below), ages of the Samples NDC-20 to NDC-27 are regarded as sometime between late Valanginian and early Barremian.

The Sample NDC-29 is characterized by the occurrence of *Pseudodictyomitra lanceoloti* which has the first appearance horizon in the late Hauterivian, and by the occurrence of *Sethocapsa* sp. aff. *S. kamigoensis* which has the last appearance horizon in the early Barremian (Baumgartner et al., 1995); these lines of evidence indicate that the age of this sample is restricted between the late Hauterivian and early Barremian.

The Sample NDC-52 yields *Pseudodictyomitra lanceoloti* and *P. leptoconica*, of which first occurrence horizon lies near the boundary between Barremian and Aptian (Baumgartner et al., 1995). Since *Acaeniotyle umbilicata*, *Wrangellium puga* and *Xitus clava* made their extinctions in Aptian time (Sanfilippo and Riedel, 1985; Ishida and Hashimoto, 1991; O'Dogherty, 1994), this sample is older than Albian. The age of the Sample NDC-52 is most probably Aptian. Occurrence of *Acaeniotyle umbilicata* from the Sample NDC-58 also suggests the age to be Aptian.

The Samples NDC-60 to NDC-172 are lacking in age-diagnostic species, and are difficult to determine the ages accurately. Although *Pseudodictyomitra lodogaensis* was first reported from the Albian to Cenomanian interval by Pessagno (1977), Ishida and Hashimoto (1991) extended the range from the Barremian. The range of *Pseudodictyomitra carpatica* is controversial among researchers. For example, Baumgartner et al. (1995) reported the range between the Kimmeridgian/Tithonian and early Barremian,

whereas Schaaf (1984) indicated its occurrence, at least, from Valanginian to Turonian. The discrepancy might result from the diverse morphotypes of this species. We also include several morphotypes into *P. carpatica* (Plate 4), and think that it is difficult to determine the age precisely by using this species. By considering these lines of data and by assuming that the section is continuous, we assign the Samples NDC-60 to NDC-172 to sometime between the Aptian and Cenomanian.

2. Radiolarians from the Shergol ophiolitic melange and their ages

We collected nine chert block samples from the Shergol ophiolitic melange near Shergol for radiolarian analysis (Fig. 2). Only one chert sample (WMRC-9; Fig. 5) yields well-preserved radiolarians. This chert is laminaceous, reddish brown in color, and is composed of cryptocrystalline quartz and radiolarian remains. The diversity of the fauna is low, but the presence of *Pseudodictyomitra pentacolaensis* makes it possible to assign this chert to the Albian (Pessagno, 1977).

Discussion

1. Age of the Nidar ophiolitic complex

The Nidar ophiolitic complex consists of ultramafic rocks, gabbro, and sedimentary-volcanic member, in ascending order (Fig. 3). The radiolarian ages of the sedimentary-volcanic member described above are consistent with the Sm-Nd mineral-whole rock isochron age (139.6 ± 32.2 Ma; Ahmad and Tanaka, in preparation) of the gabbro. This indicates that the Nidar ophiolitic complex is a series of igneous-sedimentary rock complex representing an oceanic crust covered by marine sediments.

The radiolarian ages determined in the Nidar section are, in part, based on the assumption that the section measured in this paper is continuous. The contacts between the gabbro and the volcanic-sedimentary rocks of the upper part of the measured section, however, are minor faults as shown in Fig. 4. If the lower and middle parts of the section was also deformed or repeated by faults or folds, some of the ages might be reconsidered. This possibility must be ruled out by future geologic mapping.

2. Depositional setting of the Nidar ophiolitic complex

The Nidar ophiolitic complex has an ophiolite succession, but the sedimentary-volcanic member does not show

radiolarians	Sample No.																
	NDC-16 (ch)	NDC-20 (ch)	NDC-21 (ssh)	NDC-23 (ch)	NDC-27 (ch)	NDC-29 (ch)	NDC-52 (ssh)	NDC-58 (ch)	NDC-60 (sh)	NDC-76 (sh)	NDC-83 (ssh)	NDC-122 (ssh)	NDC-123 (ssh)	NDC-160 (ssh)	NDC-169 (ssh)	NDC-172 (ssh)	WMRC-9 (ch)
<i>Acaeniotyle umbilicata</i>																	
<i>Acanthocircus trizonalis</i>			cf														
<i>Archaeospongopurum</i> spp.																	
<i>Alievium</i> spp.																	
<i>Cecrops septemporatus</i>	cf		cf		cf												
<i>Pantanellium squinaboli</i>																	
<i>Pantanellium</i> spp.																	
<i>Triactoma</i> sp.																	
<i>Hagiastrid</i>																	
<i>Cinguloturris</i> (?) sp.																	
<i>Dictyomitra pseudoscalaris</i>																	
<i>Hemicryptocapsa capita</i>																	
<i>Holocryptocanium barbui</i>																	
<i>Holocryptocanium</i> spp.																	
<i>Parvingula</i> spp.																	
<i>Pseudodictyomitra carpatica</i>																	
<i>Pseudodictyomitra lanceoloti</i>																	
<i>Pseudodictyomitra leptoconica</i>				aff													
<i>Pseudodictyomitra lodogaensis</i>																	
<i>Pseudodictyomitra nuda</i>																	
<i>Pseudodictyomitra pentacolaensis</i>																	
<i>Pseudodictyomitra</i> spp.																	
<i>Sethocapsa kamigoensis</i>							aff										
<i>Sethocapsa uterculus</i>	cf																
<i>Sethocapsa</i> spp.																	
<i>Thanarla lacrimula</i>																	
<i>Thanarla pulchra</i>																	
<i>Thanarla</i> spp.																	
<i>Turbocapsula</i> spp.																	
<i>Wrangellium puga</i>																	
<i>Xitus</i> (?) <i>alievi</i>																	
<i>Xitus clava</i>																	
<i>Xitus</i> spp.																	

Fig. 5. List of Early Cretaceous radiolarians from the Nidar ophiolitic complex in eastern Ladakh and from the chert block in the Shergol ophiolitic melange in western Ladakh. ch:chert, sh:shale, ssh:siliceous shale.

a typical oceanic plate stratigraphy, which is composed, from lower to upper, of basalt, pelagic sediments like radiolarian chert, hemipelagic sediments, and trench-fill turbidites (Matsuda and Isozaki, 1991). Instead the member consists of alternating radiolarian chert, jasperite, volcanic conglomerate, sandstone and shale, which means that the radiolarian chert was accumulated under the influence of intense volcanic activity. The occurrence of the sedimentary rocks together with the geochemical signature of volcanic rocks of the Nidar ophiolitic complex (Ahmad and Tanaka,

in preparation) strongly indicate the intra-oceanic volcanic arc origin of this complex, which is correlated with the Dras arc in western Ladakh and the Kohistan arc in Pakistan. On the other hand, the Zildat ophiolitic melange is interpreted to be formed by the subduction of Neo-Tethys ocean underneath the Eurasian plate margin (Ahmad et al., 1996). The Hauterivian to Aptian radiolarian ages reported in this paper indicate the duration of development of the Nidar volcanic arc.

Conclusions

The sedimentary-volcanic member of the Nidar ophiolitic complex in eastern Ladakh is composed of alternating chert, jasperite, volcanic rocks, red shale, volcanic conglomerate, sandstone and shale. Radiolarian assemblages from the rocks of this member in the Nidar area range in age, at least, from Hauterivian to Aptian. The radiolarian ages supported by the Sm-Nd mineral-whole rock isochron age (139.6 ± 32.2 Ma) indicate the minimum duration of development of the Nidar intra-oceanic volcanic arc. A chert block from the Shergol ophiolitic melange in western Ladakh yields Albian radiolarians.

Acknowledgments

One of the authors (T.A.) thanks the Japan Society for the Promotion of Science (JSPS) for providing long-term fellowship, which makes this joint work in Japan possible. The director of the Wadia Institute of Himalayan Geology is thanked for providing facilities for the field work.

References

- Ahmad, T., Islam, R., Khanna, P. P. and Thakur, V. C., 1996, Geochemistry, petrogenesis and tectonic significance of the basic volcanic units of the Zildat ophiolitic mélange, Indus suture zone, eastern Ladakh (India). *Geodinamica Acta (Paris)*, **1**, 222-233.
- Bagati, T. N. and Kumar, R., 1999, Evolution of sedimentary succession in Nidar ophiolitic melange in the eastern Ladakh, India. *Abstracts, XVI-Convention, Indian Assoc. Sed.*, 5-6.
- Baumgartner, P. O., O'Dogherty, L., Gorican, S., Dumitrică-Jud, R., Dumitrică, P., Pillecuit, A., Urquhart, E., Matsuoka, A., Danelian, T., Bartolini, A., Carter, E., De Wever, P., Kito, N., Marcucci, M. and Steiger, T., 1995, Radiolarian catalogue and systematics of Middle Jurassic to Early Cretaceous Tethyan genera and species. In Baumgartner, P. O., O'Dogherty, L., Gorican, S., Urquhart, E., Pillecuit, A. and De Wever, P., eds., Middle Jurassic to Lower Cretaceous Radiolaria of Tethys: Occurrences, Systematics, Biochronology. *Mémoires de Géologie (Lausanne)*, no. 23, 37-685.
- Beck, R. A., Burbank, D. W., Sercombe, W. J., Riley, G. W., Barndt, J. K., Berry, J. R., Afzal, J., Khan, A. M., Jurgen, H., Metje, J., Cheema, A., Shafique, N. A., Lawrence, R. D. and Khan, M. A., 1995, Stratigraphic evidence for an early collision between northwest India and Asia. *Nature*, **373**, 55-58.
- Clift, P. D., Degnan, P. J., Hannigan, R. and Blusztajn, J., 2000, Sedimentary and geochemical evolution of the Dras forearc basin, Indus suture, Ladakh Himalaya, India. *Geol. Soc. Am. Bull.*, **112**, 450-466.
- Dewey, J. F., Shackleton, R. M., Chang, C. F. and Sun, Y. Y., 1988, The tectonic evolution of the Tibetan Plateau. *Phil. Trans. R. Soc. Lond.*, **A327**, 379-413.
- Ishida, K. and Hashimoto, H., 1991, Radiolarian assemblages from the Lower Cretaceous formations of the Chichibu Terrane in eastern Shikoku and their ammonite ages. *Jour. Sci., Univ. Tokushima*, **25**, 23-67.*
- Matsuda, T. and Isozaki, Y., 1991, Well-documented travel history of Mesozoic pelagic chert in Japan: from remote ocean to subduction zone. *Tectonics*, **10**, 475-499.
- O'Dogherty, L., 1994, Biochronology and paleontology of Mid-Cretaceous radiolarians from Northern Apennines (Italy) and Betic Cordillera (Spain). *Mémoires de Géologie (Lausanne)*, no. 21, 415pp.
- Pessagno, E. A., Jr., 1977, Lower Cretaceous radiolarian biostratigraphy of the Great Valley Sequence and Franciscan Complex, California Coast Ranges. *Cushman Found. Foram. Res., Spec. Pub.*, no.15, 87p.
- Pessagno, E. A., Jr. and Newport, R. L., 1972, A technique for extracting Radiolaria from radiolarian cherts. *Micro-paleontology*, **18**, 231-234.
- Robertson, A. and Degnan, P., 1994, The Dras arc complex: lithofacies and reconstruction of a Late Cretaceous oceanic volcanic arc in the Indus Suture Zone, Ladakh Himalaya. *Sed. Geol.*, **92**, 117-145.
- Rowley, D.B., 1996, Age of initiation of collision between India and Asia: A review of stratigraphic data. *Earth Planet. Sci. Let.*, **145**, 1-13.
- Sanfilippo, A. and Riedel, W.R., 1985, Cretaceous radiolaria. In Bolli, H.M., Saunders, J.B. and Perch-Nielsen, K., eds., *Plankton stratigraphy*. Cambridge Univ. Press, Cambridge, 573-630.
- Schaaf, A., 1981, Late Early Cretaceous Radiolaria from Deep Sea Drilling Project Leg 62. *Init. Rep. DSDP*, **62**, 419-470.
- Schaaf, A., 1984, Les radiolaires du Crétacé inférieur et moyen: biologie et systématique. *Sci. géol. (Strasbourg) Mém.*, no. 75, 1-189. (in French with English abstract)

- Searle, M. P., 1991, Geology and Tectonics of the Karakoram Mountains. *John Wiley & Sons, Chichester*, 358p.
- Searle, M. P., Khan, A., Fraser, J. E. and Gough, S. J., 1999, The tectonic evolution of the Kohistan-Karakoram collision belt along the Karakoram Highway transect, north Pakistan. *Tectonics*, **18**, 929 - 949.
- Shah, S. K. and Sharma, M. L., 1977, A preliminary report on the fauna in radiolarites of ophiolite-mélange zone around Mulbekh, Ladakh. *Current Sci.*, **46**, 817.
- Sinha, A. K. and Mishra, M., 1992, Plume activity and sea-mounts in Neotethys: evidence supported by geochemical and geochronological data. *Jour. Himalayan Geol.*, **3**, 91-96.
- Sinha, A. K. and Upadhyay, R., 1993, Mesozoic neo-tethyan pre-orogenic deep marine sediments along the Indus-Yarlung Suture, Himalaya. *Terra Nova*, **5**, 271-281.
- Thakur, V. C., 1981, Regional framework and geodynamic evolution of the Indus-Tsangpo suture zone in the Ladakh Himalayas. *Trans. Royal Soc. Edinburgh: Earth Sci.*, **72**, 89 - 97.
- Upadhyay, R. and Sinha, A. K., 1998, Tectonic evolution of Himalayan Tethys and subsequent Indian plate subduction along Indus Suture Zone. *PINSA*, **64A**, 659-683.
- *: in Japanese with English abstract

Explanation of Plates

Plate 1 Early Cretaceous radiolarians from the Ladakh Himalaya, northern India. The numbers in parentheses indicate the sequential number of SEM photomicrograph and the rock specimen number (see explanations in the text). Scale bar is 0.24 mm for the figure 9, 0.14 mm for the figures 1, 5-8 and 10-12, and 0.1 mm for the figures 2-4 and 13.

Fig. 1. *Archaeospongoprimum* sp. (183/NDC-16). Fig. 2. *Archaeospongoprimum* sp. (378/NDC-123). Fig. 3. *Pantanellium squinaboli* (180/NDC-16). Fig. 4. *Pantanellium* sp. (346/NDC-172). Fig. 5. *Acaeniotyle umbilicata* (190/NDC-29). Fig. 6. *Acaeniotyle umbilicata* (189/NDC-29). Fig. 7. *Acaeniotyle umbilicata* (308/NDC-23). Fig. 8. *Cecrops* sp. cf. *C. septemporatus* (426/NDC-27). Fig. 9. Hagiastrid gen. and sp. indet. (363/NDC-172). Fig. 10. *Triactoma* sp. (223/NDC-29). Fig. 11. *Acanthocircus* sp. cf. *A. trizonalis* (309/NDC-23). Fig. 12. Nassellaria gen. and sp. indet. (327/NDC-23). Fig. 13. *Alievium* sp. (307/NDC-23).

Plate 2 Early Cretaceous radiolarians from the Ladakh Himalaya, northern India. The numbers in parentheses indicate the sequential number of SEM photomicrograph and the rock specimen number (see explanations in the text). Scale bar is 0.14 mm for the figures 4, 6 and 9, 0.1 mm for the figures 1, 3, 5, 7, 8 and 10-16, and 0.067 mm for the figure 2.

Fig. 1. *Holocryptocanium barbui* (250/NDC-76). Fig. 2. *Holocryptocanium barbui* (495/WMRC-9). Fig. 3. *Holocryptocanium barbui* (408/NDC-21). Fig. 4. *Holocryptocanium barbui* (184/NDC-16). Fig. 5. *Holocryptocanium barbui* (454/NDC-52). Fig. 6. *Holocryptocanium* sp. (306/NDC-23). Fig. 7. *Holocryptocanium* sp. (240/NDC-29). Fig. 8. *Holocryptocanium* sp. (202/NDC-29). Fig. 9. *Sethocapsa* sp. (214/NDC-29). Fig. 10. *Sethocapsa uterculus* (313/NDC-23). Fig. 11. *Sethocapsa uterculus* (310/NDC-23). Fig. 12. *Sethocapsa* sp. aff. *S. kamigoensis* (215/NDC-29). Fig. 13. *Sethocapsa* sp. (489/WMRC-9). Fig. 14. *Cryptamphorella* sp. (312/NDC-23). Fig. 15. *Sethocapsa* sp. (173/NDC-16). Fig. 16. *Hemicryptocapsa capita* (172/NDC-16)

Plate 3 Early Cretaceous radiolarians from the Ladakh Himalaya, northern India. The numbers in parentheses indicate the sequential number of SEM photomicrograph and the rock specimen number (see explanations in the text). Scale bar is 0.14 mm for the figures 1, 11, 13 and 14, 0.1 mm for the figures 3-10, 12, 15 and 16, and 0.067 mm for the figure 2.

Fig. 1. *Pseudodictyomitra pentacolaensis* (486/WMRC-9). Fig. 2. *Pseudodictyomitra lodogaensis* (294/NDC-169). Fig. 3. *Pseudodictyomitra lodogaensis* (480/NDC-122). Fig. 4. *Pseudodictyomitra lodogaensis* (479/NDC-122). Fig. 5. *Pseudodictyomitra lodogaensis* (295/NDC-169). Fig. 6. *Pseudodictyomitra lodogaensis* (301/NDC-169). Fig. 7. *Pseudodictyomitra* sp. (274/NDC-76). Fig. 8. *Pseudodictyomitra* sp. (262/NDC-76). Fig. 9. *Xitus clava* (325/NDC-23). Fig.

10. *Xitus clava* (232/NDC-29). Fig. 11. *Xitus* (?) *alievi* (229/NDC-29). Fig. 12. *Xitus clava* (228/NDC-29). Fig. 13. *Xitus* (?) *alievi* (230/NDC-29). Fig. 14. *Xitus clava* (449/NDC-52). Fig. 15. *Parvicingula* sp. (122/NDC-16). Fig. 16. *Cinguloturris* (?) sp. (492/WMRC-9)

Plate 4 Early Cretaceous radiolarians from the Ladakh Himalaya, northern India. The numbers in parentheses indicate the sequential number of SEM photomicrograph and the rock specimen number (see explanations in the text). Scale bar is 0.14 mm for the figures 5, 6, 8, 9, 11, 13 and 14, and 0.1 mm for the figures 1-4, 7, 10 and 12.

Fig. 1. *Pseudodictyomitra lanceoloti* (448/NDC-52). Fig. 2. *Pseudodictyomitra lanceoloti* (269/NDC-76). Fig. 3. *Pseudodictyomitra lanceoloti* (508/NDC-83). Fig. 4. *Pseudodictyomitra lanceoloti* (193/NDC-29). Fig. 5. *Pseudodictyomitra carpatica* (201/NDC-29). Fig. 6. *Pseudodictyomitra carpatica* (368/NDC-123). Fig. 7. *Pseudodictyomitra* sp. aff. *P. leptoconica* (334/NDC-23). Fig. 8. *Pseudodictyomitra carpatica* (155/NDC-16). Fig. 9. *Pseudodictyomitra carpatica* (507/NDC-83). Fig. 10. *Wrangellium puga* (475/NDC-52). Fig. 11. *Wrangellium puga* (147/NDC-16). Fig. 12. *Pseudodictyomitra leptoconica* (451/NDC-52). Fig. 13. *Wrangellium puga* (125/NDC-16). Fig. 14. *Wrangellium* sp. (156/NDC-16). Fig. 15. *Pseudodictyomitra nuda* (414/NDC-21)

Plate 5 Early Cretaceous radiolarians from the Ladakh Himalaya, northern India. The numbers in parentheses indicate the sequential number of SEM photomicrograph and the rock specimen number (see explanations in the text). Scale bar is 0.14 mm for the figure 4, and 0.1 mm for the figures 1-3 and 5-11.

Fig. 1. *Dictyomitra pseudoscalaris* (186/NDC-16). Fig. 2. *Dictyomitra pseudoscalaris* (158/NDC-16). Fig. 3. *Dictyomitra pseudoscalaris* (121/NDC-16). Fig. 4. *Dictyomitra pseudoscalaris* (246/NDC-29). Fig. 5. *Dictyomitra pseudoscalaris* (210/NDC-29). Fig. 6. *Dictyomitra pseudoscalaris* (261/NDC-76). Fig. 7. *Thanarla* sp. (485/WMRC-9). Fig. 8. *Thanarla pulchra* (245/NDC-29). Fig. 9. *Thanarla* sp. (473/NDC-52). Fig. 10. *Thanarla lacrimula* (512/NDC-83). Fig. 11. *Turbocapsula* sp. (252/NDC-76)

Plate 1

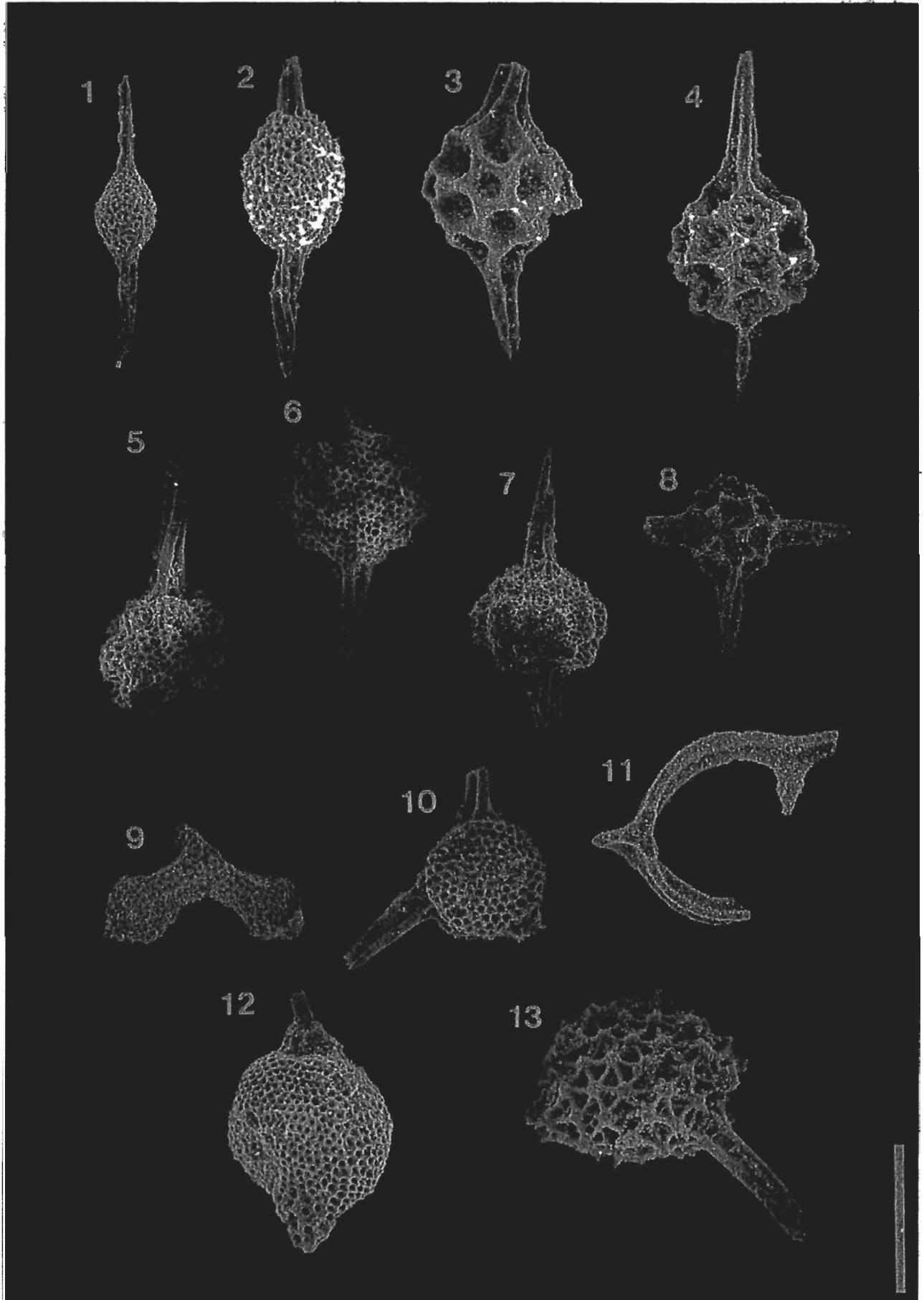


Plate 2

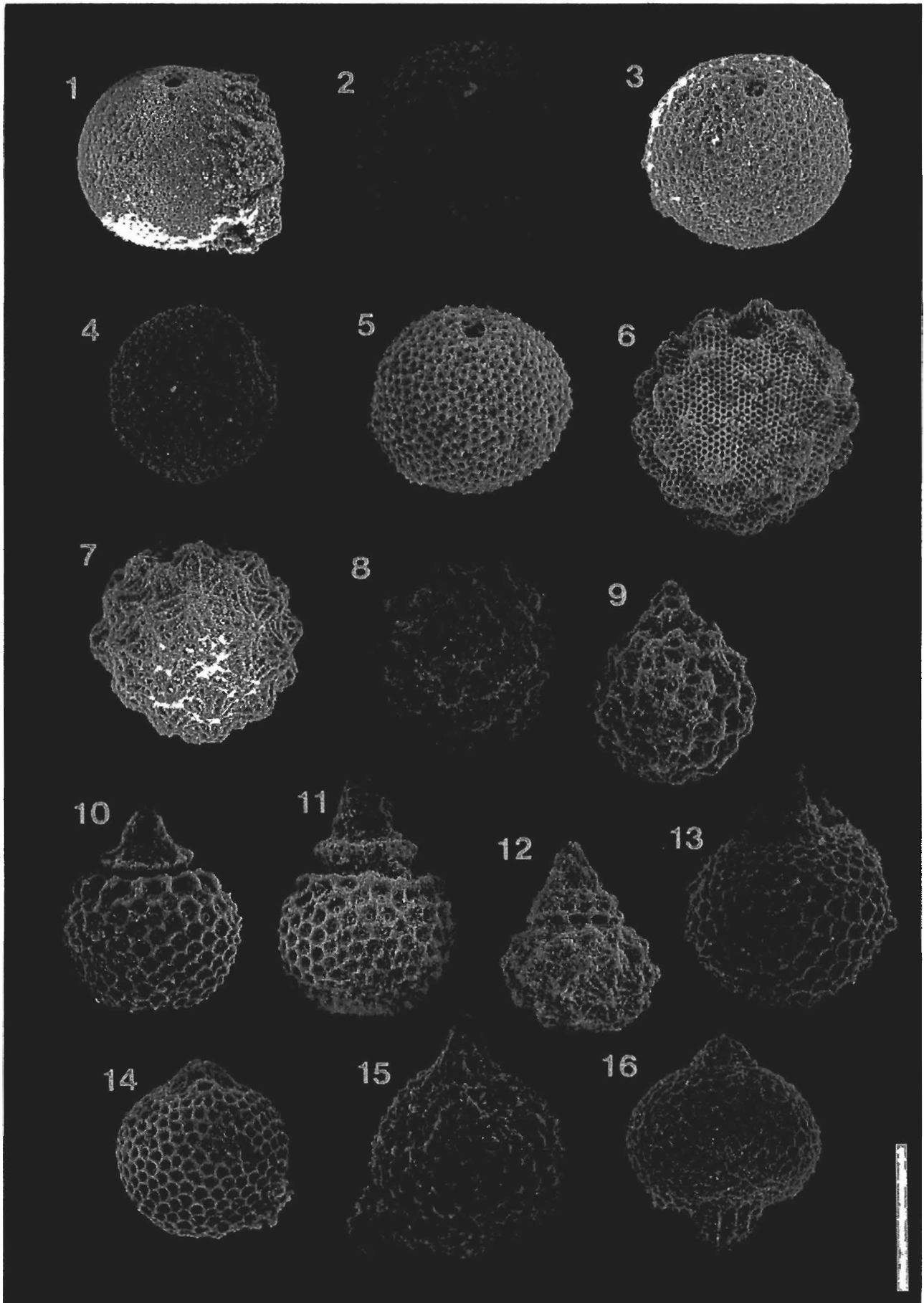


Plate 3

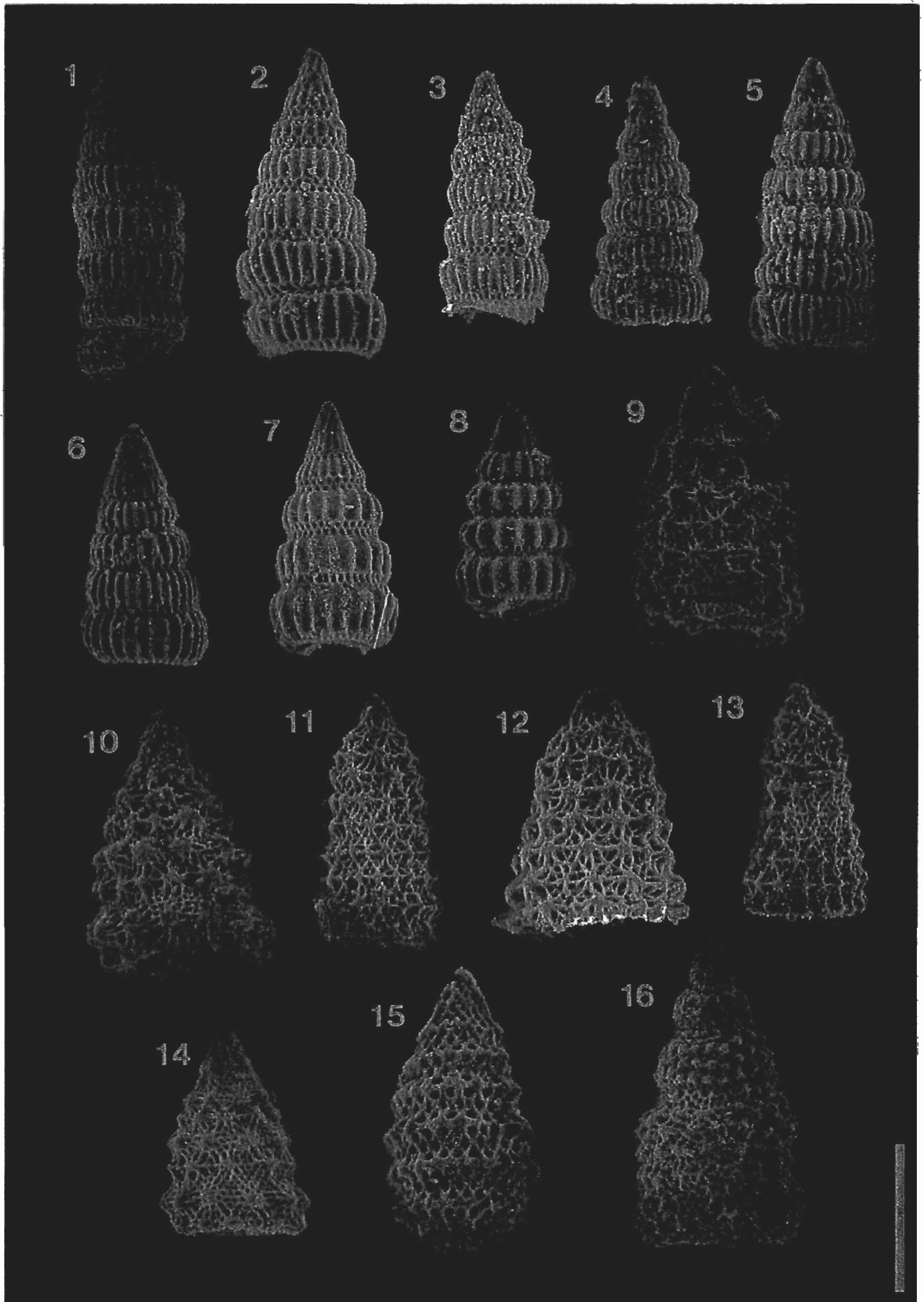


Plate 4

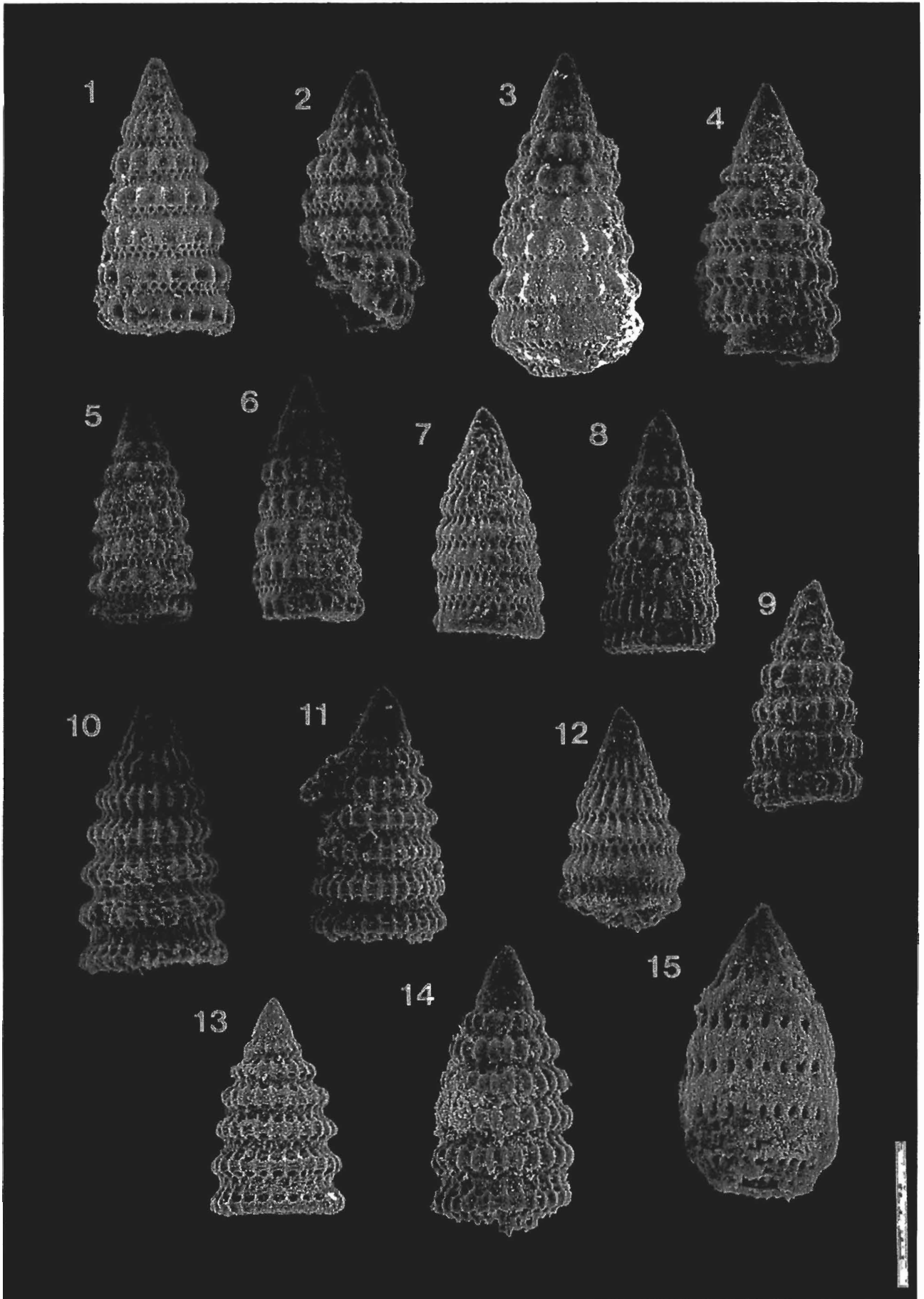


Plate 5

